

In situ imaging of the mouse cochlea using two-photon microscopy

Xin Yang¹, Ye Pu¹, Demetri Psaltis¹ and Konstantina M. Stankovic²

¹Ecole Polytechnique Federale de Lausanne, Lausanne, Switzerland

²Harvard Medical School, Department of Otology and Laryngology and Massachusetts Eye and Ear Infirmary, Department of Otolaryngology, Boston, Massachusetts

ABSTRACT

Intracochlear imaging is of great interest clinically because cochlea is the central organ of hearing. However, intracochlear imaging is technologically challenging due to the cochlea's small size and encasement in bone. The state-of-the-art imaging techniques are not adequate for high resolution cellular imaging to establish diagnosis without destroying the cochlea. We report in situ imaging of intact mouse cochlea using endogenous two-photon excitation fluorescence (TPEF) as the contrast mechanism. TPEF eliminates the need for exogenous labeling and eradicating the staining-induced artifacts. We used a natural, membranous opening into the cochlea, the round window, as the optical access to reach the organ of Corti, requiring no additional slicing or opening. Our approach provides the maximum non-invasiveness in the imaging process. TPEF exhibits strong contrast allowing deep imaging of mouse cochlea with cellular and even subcellular resolution. Inner hair cell, outer hair cell and supporting cell are clearly identifiable in TPEF images. Distinct morphological differences are observed between healthy and noise-exposed cochleae, allowing detection of specific, noise-induced pathologic changes. The TPEF images taken through the round window are correlated with the whole mount sections, verifying their reliability. Compared with one-photon excitation fluorescence (OPEF) confocal microscope and wide-field transmission microscope images taken under the same magnification and resolution, TPEF images demonstrate clear advantages in terms of sharpness, signal to noise ratio and contrast. These capabilities provide a working foundation for microendoscopy-based clinical diagnostics of sensorineural hearing loss.

Keywords: two photon microscopy, cochlea, diagnosis, noise trauma

1. INTRODUCTION

Sensorineural hearing loss (SNHL) affects the mechanosensory and neural structures of the inner ear. Due to the inadequate in-vivo imaging techniques nowadays, the research toward understanding the cellular basis of SNHL is limited to histological studies, which cannot be done without destroying hearing, and are based on examination of cadaveric tissue. Consequently, the cellular basis of SNHL in any given person is typically unknown. Computed tomography (CT) and magnetic resonance imaging (MRI) are two major in-vivo imaging techniques widely used clinically. They are crucial in deep tissue imaging and valuable in diagnosis of pathological changes. However, due to the poor resolution, they are inadequate for inner ear imaging to establish cellular diagnosis. Additionally, the complex three dimensional structure, encasement in the densest bone in the body, and small size of the inner ear add up to the difficulties of intracochlear imaging. Fortunately, there are two natural openings into the inner ear: the round and oval windows, and most hearing loss starts and is most prominent in the region close to the round window. Access through the round window offers the opportunity to discover the unknown cochlea; this access has been used for vibratory transducer implants¹, intra-tympanic drug delivery² and cochlear implants³.

Optical techniques are particularly well suited for imaging of the delicate intracochlear structures because they offer a significantly higher spatial resolution and lower cost compared to CT and MRI scans. Confocal microscopy⁴ and optical coherence tomography^{5,6} have been applied to the cochlea. Confocal microscopy is advantageous for its high resolution and deep penetration depth, yet disadvantageous for the necessity of exogenous labeling. The exogenous dyes or antibodies may result in tissue deformation and artifacts, thus limiting interpretation of the results. Compared with traditional confocal microscopy, two-photon excitation fluorescence (TPEF) microscopy⁷ is a more appropriate technique for deep-tissue imaging. It provides a much deeper penetration, reduced photo-damage, and improved detection sensitivity while maintaining a spatial resolution comparable with confocal microscopy⁸⁻¹².

In this paper, endogenous TPEF and second harmonic generation (SHG) are used as the contrast mechanisms to image intracochlear cells, including sensory hair cells and cochlear neurons. No exogenous staining is introduced, minimizing the possible artifacts. The round window is used as the optical access without any additional physical openings. High

quality images with cellular level resolution are obtained, from which sufficient diagnosis of morphological defects can be established. The TPEF images show clear advantages over traditional confocal images, leading to a great potential for new and efficient diagnostic tool for hearing loss.

2. METHOD

2.1 Animals handling

Thirty four male mice (CBA/CaJ strains) were used in this study, of which 12 were exposed to an octave band noise of 8-16 kHz at 106 dB SPL for 2h, and 22 served as unexposed controls. Noise exposure was chosen to cause permanent cellular damage, leading to marked morphological changes in sensory cells.

All animal procedures were approved by the Animal Care and Use Committee of the Massachusetts Eye and Ear Infirmary and Ecole Polytechnique Federale de Lausanne.

2.2 Cochlear extraction and whole mount preparation

Twelve noise exposed mice and 12 control mice were sacrificed two weeks after noise exposure, to mimic a common clinical scenario when patients seek help several weeks after the trauma. The animals were intracardially perfused with 4% paraformaldehyde in 0.1M phosphate buffer. The left inner ears were extracted, stored in 4% paraformaldehyde at room temperature¹³, and imaged within a week of harvest to ensure a strong signal. The right ears were dissected as whole-mount sections and stained with phalloidin conjugated with Alexa-568, which targets F-actin in the stereocilia, and TOPRO-3, which targets cell nuclei¹⁴.

Ten additional control mice were sacrificed and their cochleae were extracted without using intracardiac or intracochlear fixatives. These unstained cochleae were imaged within 5 minutes of extraction.

2.3 Two Photon Microscopy of the Cochlea in situ

The extracted cochleae were mounted in an elastic mould made of 1% agarose in water, and oriented with the round window facing the microscope objective.

The two-photon images were acquired using a Leica SP5 multiphoton microscope system. The excitation wavelength was 812 nm and TPEF and SHG were collected at 525 nm (50 nm bandwidth) and 406 nm (10 nm bandwidth), respectively, through two separate photon multiplier tubes (PMT) equipped with the corresponding bandpass filters.

Traditional one-photon confocal microscopy images were taken with a Zeiss LSM 700, using the excitation wavelength of 406 nm (equivalent to 812 nm excitation in the TPEF case), and detecting the emission wavelength of 500-550 nm. Wide-field transmission images were taken with the same system under a different mode.

3. RESULTS AND DISCUSSIONS

As discussed earlier, TPEF has intrinsic advantages over traditional one-photon excitation fluorescence confocal microscopy (OPEF) in terms of penetration depth, optical sectioning and signal to noise ratio (SNR). In order to quantify the benefit of TPEF in cochlear imaging, TPEF, OPEF and wide-field transmission images were taken through the round window under the same orientation, magnification, and resolution (~350nm). The images are displayed and compared in Fig. 1. Rows of hair cells are seen with sharp details and high SNR in the TPEF image (Fig. 1 (a)). The OPEF image demonstrates a lower SNR (Fig. 1 (b)), where the three rows of outer hair cells are barely visible with fuzzy details. The wide-field transmission image is completely blurry (Fig. 1 (c)), where only outlines of hair cells are identifiable, without any details of individual cell. This mainly results from the lack of axial resolution (optical sectioning) and strong scattering from the surrounding bone. The image contrast, defined as the ratio of the mean intensity of the hair cell region to the mean intensity of the imaging plane 10 μ m above the hair cell, are ~4 and ~2 for TPEF and OPEF images, respectively. The SNR, defined as the ratio of the mean intensity of the hair cell region to the standard deviation of the background in the peripheral area of the same imaging plane, is ~20 and ~10 for TPEF and OPEF images, respectively. The differences are mainly due to the longer excitation wavelength of TPEF, which ensures less scattering and deeper penetration, and the square dependence of excitation/emission, which allows optical sectioning.

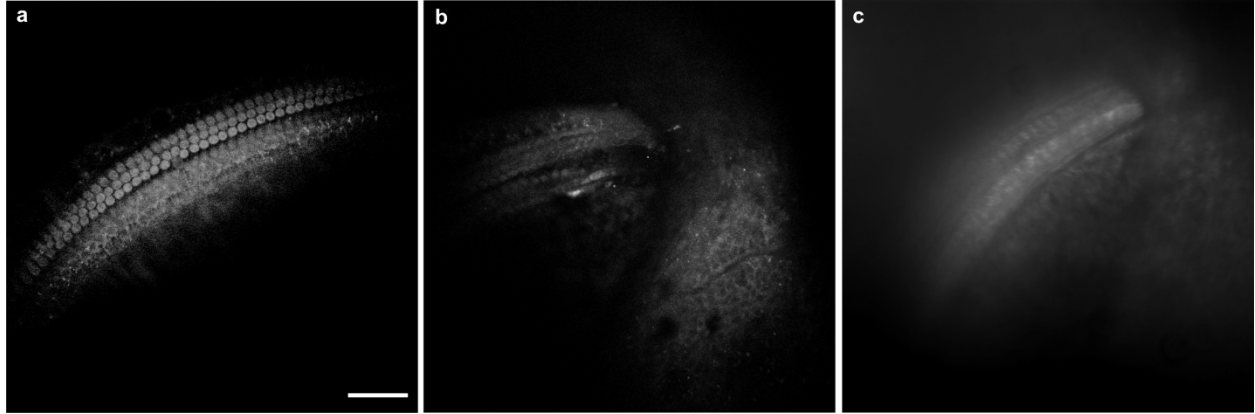


Fig. 1 Images of the organ of Corti taken through the round window using (a) TPEF microscopy, (b) OPEF microscopy and (c) wide-field transmission microscopy with the same magnification. TPEF microscopy shows better visual acuity and signal-to-noise ratio compared to the other methods. Scale bar: 50 μm .

Fig. 1 was obtained from fixed cochleae, where tissue degradation was halted, allowing sufficient time for image taking and optimization. However, for the purpose of in-vivo imaging or ex-vivo imaging that best represents the in-vivo environment, non-fixed tissue is preferred. This is important because although paraformaldehyde fixative that we used is known to be superior in preserving cell fluorescence while limiting background, it inevitably introduces certain amount of fluorescence. We therefore performed TPEF imaging of the non-fixed cochlear tissue to verify the reliability of TPEF as imaging contrast. In contrast to the fixed cochleae, the TPEF signal from the non-fixed, ex-vivo cochleae degraded quickly with time. In order to achieve similar signal intensity as from the fixed tissue, the images were taken within five minutes of the tissue harvest. Fig. 2 shows hair cells viewed through the round window at a different angle than in Fig. 1.

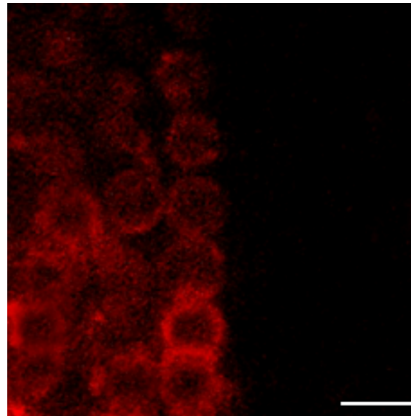


Fig. 2 A TPEF image of the organ of Corti viewed through the intact round window of an unfixed, unstained cochlea in situ. The image was taken within 5 minutes of cochlear harvest. Rows of hair cells are clearly seen, similar to those observed in Fig. 1 (a). The scale bar is 10 μm .

To demonstrate the capability of TPEF for morphological diagnosis of hearing loss, we compared the TPEF images taken through the round window of normal and noise-exposed cochleae (Fig. 3). Both normal (Fig. 3 (a)) and noise-exposed cochleae (Fig. 3 (b)) exhibited strong TPEF signal, providing satisfactory details about cell morphology. Regular and periodical rows of hair cells (asterisk: outer hair cell, arrow head: inner hair cell) are observed in normal cochlea (Fig. 3 (a)), similar to Fig. 1 (a), while outer hair cells (asterisk) are largely missing and inner hair cells (arrow head) are decimated in the noise-exposed cochlea (Fig. 3 (b)). This agrees with our expectation, and further confirms the capability of TPEF in diagnosis of hearing loss with conspicuous morphological changes.

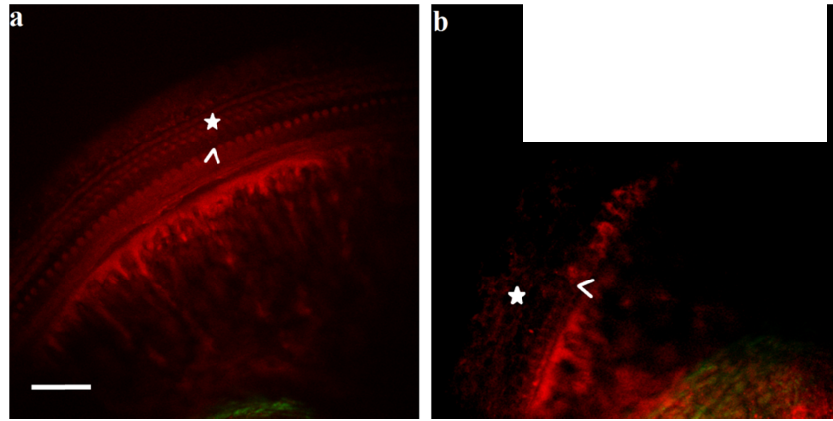


Fig. 3 Images of the organ of Corti seen through the round window of normal (a) and noise-exposed (b) cochleae. The scale bar is 50 μm . The asterisk points to the three rows of outer hair cells, which are missing in the noise-exposed cochleae. The arrowhead points to the row of inner hair cells, which are decimated after noise exposure.

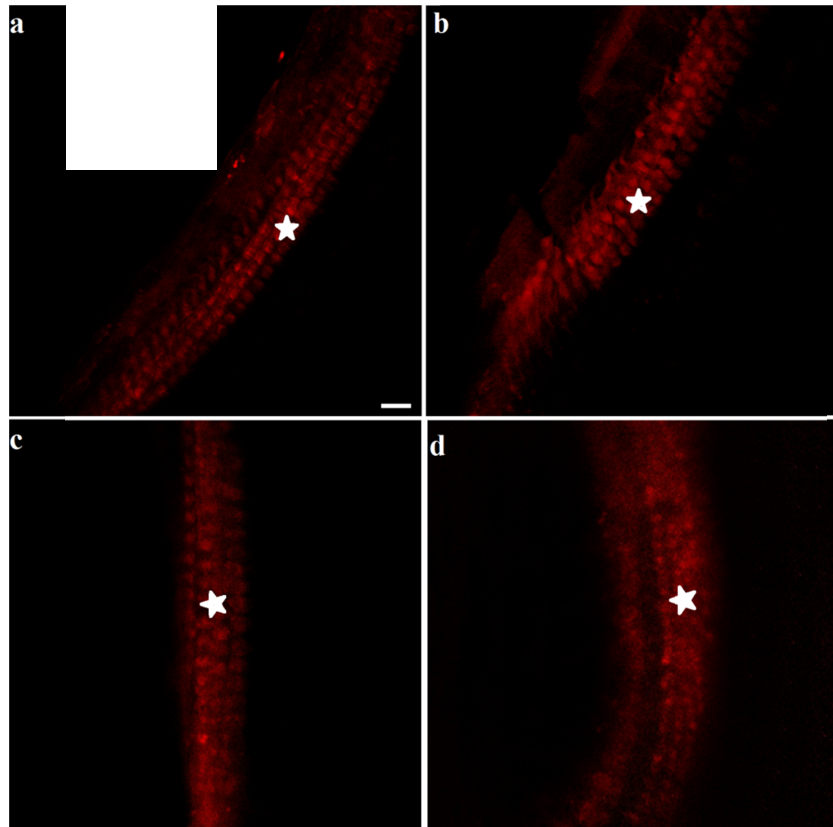


Fig. 4 Comparison of the organ of Corti of decalcified normal and noise-exposed cochleae in basal and apical turns, respectively. The scale bar is 10 μm . (a) basal turn of normal cochlea (b) basal turn of noise-exposed cochlea (c) apical turn of normal cochlea (d) apical turn of noise-exposed cochlea. The outer hair cells in basal turn are disarrayed in the noise-traumatized cochlea (b), while no noticeable changes are observed in apical turn (d).

Imaging through the round window limits diagnostics to the hook region of the organ of Corti, which is the most probable place for the initiation of the sensorineural damage. Decalcification made the cochlear bone transparent, thus allowing visualization of the basal and apical cochlear turns through the cochlear bone. To assess noise-induced damage along the length of the cochlea, the cochlear bone was decalcified in 80% Formic acid and 20% Tri-sodium citrate for 3 hours. After decalcification, the penetration depth improved from $\sim 100\text{ }\mu\text{m}$ to $\sim 2\text{ mm}$ (limited by the working distance of the microscope objective), allowing TPEF imaging of the basal and apical turns along the organ of Corti. Fig. 4 (a) and (b) compare hair cells located in the basal turns of the normal and noise-exposed cochleae. Noise exposure lead to less cellular damage in the basal turn compared to the hook region near the round window. Although the outer hair cells were disarrayed after noise trauma (Fig. 4 (b)), only a small portion of them are torn off from the basilar membrane in the basal turn. The apical turn (Fig. 4 (c-d)) of the noise-exposed cochlea (Fig. 4 (d)) demonstrates no noise-induced loss of hair cells.

The TPEF images obtained from intact cochlea were further confirmed with stained whole-mount samples. The green channel (Alexa-568) was obtained using two-photon fluorescence excited at 1000 nm wavelength, and the red channel (TO-PRO-3) was obtained using one-photon confocal microscopy with an excitation at 633 nm. Normal and noise-exposed cochlear whole-mount sections were compared (Fig. 5). The highe-frequency region close to the round window, particularly around 45.2 kHz, is most seriously damageed, which is indicated by disarrayed stereocilia and cells. Further down at 32.0 kHz region, hair cell damage is less severe. In the 11.3 kHz region the exposed cochleae appear to be almost identical with the unexposed cochleae. These observations are consistent with our TPEF imaging of unstained, intact cochleae though the round window.

TPEF microscopy was also capable of imaging cochlear neurons at the cellular level through the encasing cochlear bone instead of through the round window (Fig. 6). The TPEF channel (red) reveals the neural somata, the average size of which is $\sim 30\mu\text{m}$, approximately four to five times bigger than the hair cells. This leads to an opportunity to diagnose hearing problems of neural origin.

4. CONCLUSION

We have investigated TPEF imaging through the round window of the mouse cochlea as a potential diagnostic tool for sensorineural hearing loss. The use of TPEF eliminates the need for exogenous labeling and provides the maximum non-invasiveness in the process. We find that TPEF is advantageous over OPEF and wide-field transmission microscopy. Our experiments reveal fine cellular structure of the hair cells, and allow morphological distinction between healthy and damaged organs of Corti, consistent with imaging of the stained whole mounts. Combined, these capabilities provide a working foundation for microendoscopy-based clinical diagnostics of sensorineural hearing loss.

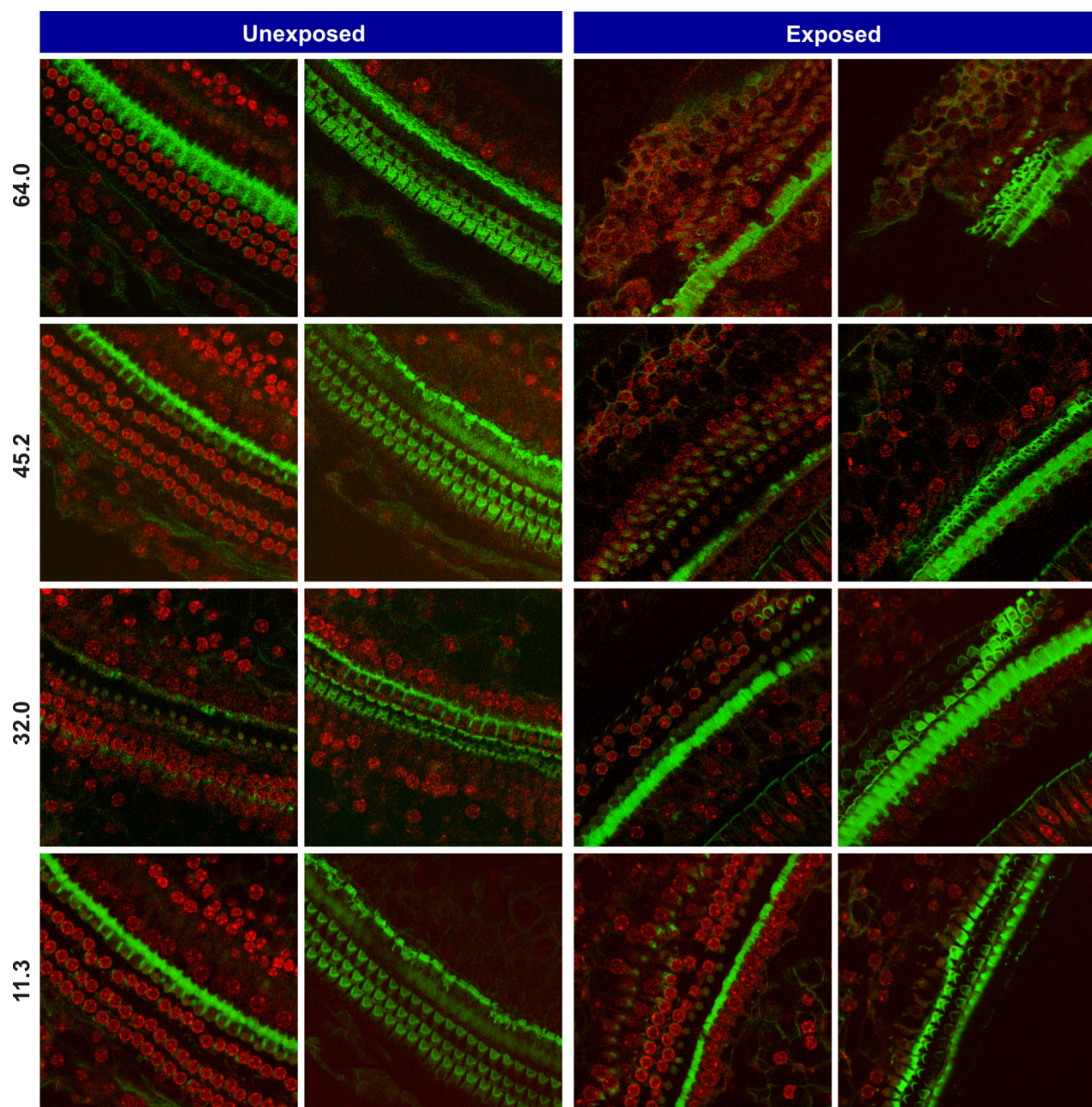


Fig. 5 Images of mouse cochlear whole-mounts stained with Alexa-conjugated phalloidin (green channel, for stereocilia) and TO-PRO-3 (red channel, for cell nucleus). In both columns, the left panels display the layer containing the nucleus of the hair cells while the right panels show the layer containing stereocilia. The number to the left of the rows indicates the corresponding frequency locations (in kHz) along the length the cochlea.

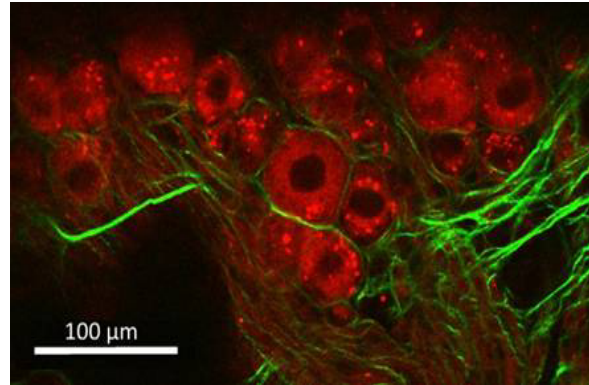


Fig. 6 A TPEF image of cochlear neurons under intact bone. The red channel is TPEF, which reveals the neural somata. The green channel is endogenous SHG, which possibly originates from the myelinated nerve fibers (white arrows). Intracellular organelles (white arrow heads) and cell nuclei (asterisk) can be seen in neurons. The scale bar is 100 μ m.

ACNOWLEDGEMENT

We are grateful for the support of the Bertarelli Foundation.

REFERENCES

- [1] V. Colletti, S. D. Soli, M. Carner and L. Colletti, "Treatment of mixed hearing losses via implantation of a vibratory transducer on the round window," *Int J Audiol* 45(10), 600-608 (2006)
- [2] A. N. Salt and Y. L. Ma, "Quantification of solute entry into cochlear perilymph through the round window membrane," *Hearing Res* 154(1-2), 88-97 (2001)
- [3] B. Mangus, A. Rivas, B. S. Tsai, D. S. Haynes and J. T. Roland, "Surgical Techniques in Cochlear Implants," *Otolaryng Clin N Am* 45(1), 69-78 (2012)
- [4] G. H. MacDonald and E. W. Rubel, "Three-dimensional imaging of the intact mouse cochlea by fluorescent laser scanning confocal microscopy," *Hear Res* 243(1-2), 1-10 (2008)
- [5] F. Y. Chen, N. Choudhury, J. F. Zheng, S. Matthews, A. L. Nutall and S. L. Jacques, "In vivo imaging and low-coherence interferometry of organ of Corti vibration," *J Biomed Opt* 12(2), (2007)
- [6] B. J. F. Wong, J. F. de Boer, B. H. Park, Z. P. Chen and J. S. Nelson, "Optical coherence tomography of the rat cochlea," *J Biomed Opt* 5(4), 367-370 (2000)
- [7] W. Denk, J. H. Strickler and W. W. Webb, "2-Photon Laser Scanning Fluorescence Microscopy," *Science* 248(4951), 73-76 (1990)
- [8] A. Monfared, N. H. Blevins, E. L. M. Cheung, J. C. Jung, G. Popelka and M. J. Schnitzer, "In vivo Imaging of mammalian cochlear blood flow using fluorescence microendoscopy," *Otology & Neurotology* 27(2), 144-152 (2006)
- [9] P. T. C. So, C. Y. Dong, B. R. Masters and K. M. Berland, "Two-photon excitation fluorescence microscopy," *Annual Review of Biomedical Engineering* 2, 399-429 (2000)
- [10] B. G. Wang, K. Konig and K. J. Halbhuter, "Two-photon microscopy of deep intravital tissues and its merits in clinical research," *Journal of Microscopy-Oxford* 238(1), 1-20 (2010)
- [11] W. R. Zipfel, R. M. Williams and W. W. Webb, "Nonlinear magic: multiphoton microscopy in the biosciences," *Nature Biotechnology* 21(11), 1368-1376 (2003)
- [12] X. Yang, Y. Pu, C. L. Hsieh, C. A. Ong, D. Psaltis, K. M. Stankovic, "Two-photon microscopy of the mouse cochlea in situ for cellular diagnosis," *J Biomed Opt* 18(3), 031104-11 (2013)
- [13] K. Stankovic, C. Rio, A. P. Xia, M. Sugawara, J. C. Adams, M. C. Liberman and G. Corfas, "Survival of adult spiral ganglion neurons requires erbB receptor signaling in the inner ear," *J Neurosci* 24(40), 8651-8661 (2004)
- [14] R. R. Taylor, G. Nevill, and A. Forge, "Rapid Hair Cell Loss: A Mouse Model for Cochlear Lesions," *J Assoc Res Otolaryngol*. 9(1), 44-64 (2008)